Title
Observations of the thermal environment on Red Sea platform reefs: a heat budget analysis

Journal
Coral Reefs, 30(Suppl 1)

ISSN
0722-4028

Authors
Davis, KA
Lentz, SJ
Pineda, J
et al.

Publication Date
2011-06-01

DOI
10.1007/s00338-011-0740-8

Coral Reefs (2011) 30:25–36
DOI 10.1007/s00338-011-0740-8

REPORT

Observations of the thermal environment on Red Sea platform reefs: a heat budget analysis

K. A. Davis · S. J. Lentz · J. Pineda · J. T. Farrar · V. R. Starczak · J. H. Churchill

Received: 31 October 2010 / Accepted: 21 February 2011 / Published online: 11 March 2011

Abstract Hydrographic measurements were collected on nine offshore reef platforms in the eastern Red Sea shelf region, north of Jeddah, Saudi Arabia. The data were analyzed for spatial and temporal patterns of temperature variation, and a simple heat budget analysis was performed with the goal of advancing our understanding of the physical processes that control temperature variability on the reef. In 2009 and 2010, temperature variability on Red Sea reef platforms was dominated by diurnal variability. The daily temperature range on the reefs, at times, exceeded 5°C—as large as the annual range of water temperature on the shelf. Additionally, our observations reveal the proximity of distinct thermal microclimates within the bounds of one reef platform. Circulation on the reef flat is largely wave driven. The greatest diurnal variation in water temperature occurs in the center of larger reef flats and on reefs protected from direct wave forcing, while smaller knolls or sites on the edges of the reef flat tend to experience less diurnal temperature variability. We found that both the temporal and spatial variability in water temperature on the reef platforms is well predicted by a heat budget model that includes the transfer of heat at the air–water interface and the advection of heat by currents flowing over the reef. Using this simple model, we predicted the temperature across three different reefs to within 0.4°C on the outer shelf using only information about bathymetry, surface heat flux, and offshore wave conditions.

Keywords Heat budget · Temperature variability · Red Sea · Platform reef · Reef circulation

Communicated by Guest Editor Dr. Clifford Hearn

K. A. Davis · S. J. Lentz · J. T. Farrar · J. H. Churchill
Department of Physical Oceanography, Woods Hole Oceanographic Institution, Woods Hole, MA 02543, USA

K. A. Davis (✉) · J. Pineda · V. R. Starczak
Biology Department, Woods Hole Oceanographic Institution, Woods Hole, MA 02543, USA
e-mail: kadavis@whoi.edu

Introduction

Coral reefs typically thrive in environments characterized by a high degree of thermal stability (Hoegh-Guldberg 1999). Rising sea surface temperatures due to global climate change are a severe threat to coral reefs, as reef corals live near their upper thermal limits (Goreau et al. 2000; Guinotte et al. 2003; Cantin et al. 2010). Coral bleaching is the loss of pigmentation due to the breakdown of symbiosis between reef-building corals and their symbiotic algae (zooxanthellae). Elevated temperature is the primary cause of mass coral bleaching events (Glynn 1993), but recent work also suggests that organismal response to temperature variation is complex; it can depend on other biological and physiochemical factors such as the history of thermal exposure, ability to adapt or acclimate to thermal changes, short-term temperature variability, water flow, heterotrophic feeding, and light (Nakamura and van Woesik 2001; Berkelmans 2002; Lesser et al. 2004; McClanahan et al. 2005; Sammarco et al. 2006; Palardy et al. 2008; Weller et al. 2008). These factors contribute to the high degree of spatial variability in coral bleaching observed at global, regional, and even individual reef scales (Riegl and Piller 2003; McClanahan et al. 2005).

The work presented here was inspired by observations revealing distinct thermal microclimates on table reef platforms on the Saudi coast of the Red Sea during a shelf-wide

circulation study from October 2008 to May 2010. Temperature variability on the Red Sea reef platforms is strongly diurnal, and as we show below, the daily temperature range can vary drastically across the reef. For example, a coral on the wave-exposed side of the reef, which is regularly flushed with water from the shelf, may experience a diurnal water temperature range of 0.5–1.5°C, while colonies of the same species in the interior or wave-protected side of the reef platform, approximately 200 m away, experience a 2–5°C diurnal range. Spatial patterns in temperature variation on reefs have been shown to influence the distribution of stress-tolerant coral symbionts (Glynn et al. 2001) and, recently, much attention has focused on the potential for corals to increase their thermal tolerance through a shift to more stress-tolerant symbiont assemblages (Buddemeier and Fautin 1993; Jones et al. 2008a, b; Oliver and Palumbi 2009). The history of local environmental conditions on a reef can influence the acclimation and adaptation of corals to extreme thermal events (Riegl and Piller 2003). To improve our understanding of the role that local environmental conditions play in coral bleaching and mortality, it is crucial to have a detailed understanding of the physical processes that shape the hydrodynamic and thermal environment on reefs.

Nadaoka et al. (2001) conducted a month-long observational study on a fringing reef in Okinawa and found that spatial variability in water temperature was influenced by atmospheric conditions and the horizontal advection of water from a river plume and from offshore of the reef. Similar results were found by Smith (2001) in a study of heat fluxes on a Bahamian reef during a bleaching event in July and August 1990. Smith (2001) found that anomalously high water temperature during the bleaching episode was due to a combination of low winds, which reduced evaporative cooling, and the advection of warm water onto the reef from both along- and across-shelf currents. Schiller et al. (2009) used ocean reanalysis data to examine the dynamical drivers of sea surface temperature (SST) anomalies in the Coral Sea and Great Barrier Reef. The authors found that mean horizontal advection largely controls SST in the region for most of the year, but that eddy-induced heat flux becomes important during extreme SST anomalies.

In a study of coral health and recovery after the worldwide 1998 coral bleaching event, Riegl and Piller (2003) suggested that the upwelling of cool, deep water onto reefs in the Bahamas and South Africa may be responsible for the reduced bleaching observed at these locations. Vertical mixing driven by wind stress and tidal flows around reefs can also act to cool down surface water and may be another factor responsible for the spatial variability observed in thermal stress on reefs (Bird 2005; Skirving et al. 2006).

These studies identify several mechanisms that influence the thermal environment on reefs, but observational work in this area is limited to studies with relatively short time series (Nadaoka et al. 2001; Smith 2001) or those without local meteorological measurements (Bird 2005) forcing them to rely on surface heat fluxes calculated from distant meteorological data or from model or satellite-derived products which can have large uncertainties. Here, we use a 20-month record of meteorological conditions, currents, and water temperatures to examine temporal and spatial patterns of temperature variation on Red Sea platform reefs and the surrounding shelf and to perform a simple heat budget analysis with the goal of advancing our understanding of the physical processes that shape the thermal environment on the reef. Additionally, these measurements are of value because there are few time series of oceanographic and meteorological properties in this region that can be used to characterize the physical conditions on the Red Sea reef systems.

Measurements and methodology

Field site description

Hydrographic measurements were collected on offshore reef platforms in the eastern Red Sea shelf region, north of Jeddah, Saudi Arabia (Fig. 1a). The climate in this region is arid, with strong evaporation ($\sim$2 m year^{-1}) and very little precipitation or river runoff (Sofianos and Johns 2002). In the northern part of the Red Sea (north of 19–20°N), winds are primarily from the northwest throughout the year (Fig. 1a), modified by a strong diurnal land–sea breeze cycle in the coastal regions and, in the winter, by a series of westward-blowing mountain gap wind jets along the Saudi Arabian coast (Jiang et al. 2009). Tidal currents in the central and northern Red Sea are mixed semi-diurnal and are weak (Sofianos and Johns 2007).

The coral reefs in the vicinity of Jeddah are classified as either fringing reefs or offshore reef platforms (Montaggioni et al. 1986). Fringing reefs line the shore and typically have a reef flat and steep reef slope area on the offshore side but can also have shallow lagoons between the reef and shore with coral knobs and patches. Farther offshore, reef platforms rise from the sandy shelf bottom (depth $\sim$20–50 m) to within a meter of the surface with reef flats composed of coral rubble and scattered live coral colonies (predominantly *Stylophora pistillata*) and steeply sloping flanks on all sides that are more densely populated with a diverse assemblage of corals including *Pocillopora* spp., *Porites* spp., *Acropora* spp., *Millepora* spp., and *Platygyra* spp. and coralline algae. The offshore reef platforms can vary in size and shape from submerged coral patches ($\sim$10 m^2) to coral knolls ($\sim 10^3$ m^2) to elongate or crescentic table reefs ($\sim 10^5$–10^6 m^2) (Montaggioni et al.

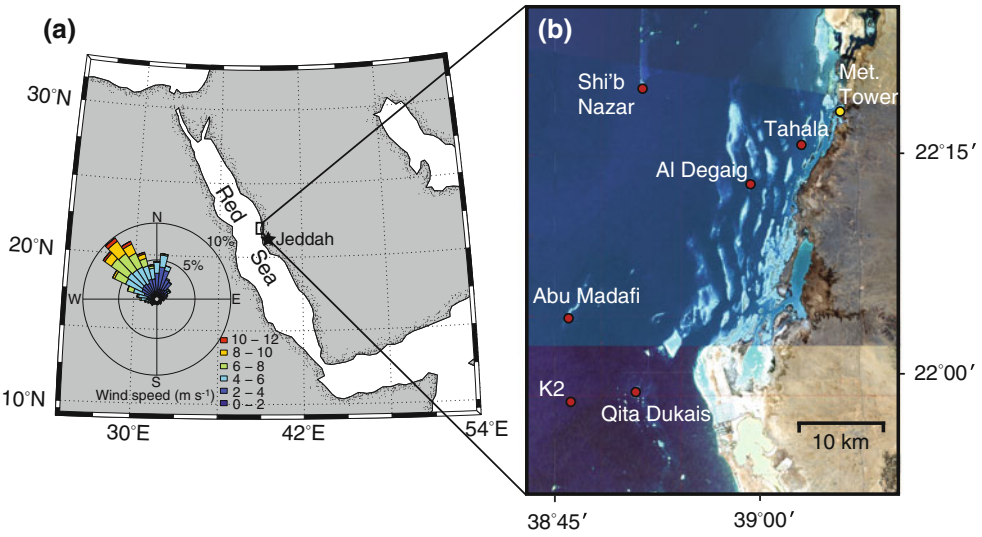

Fig. 1 **a** Regional map of study location and windrose showing the direction (from which wind blows) and magnitude of winds measured from October 2008 through October 2009 at the meteorological buoy and **b** USGS LandSAT image of study area. Mooring locations are indicated with red circles, and the meteorological tower is indicated with a yellow circle. The meteorological buoy is approximately 30 km offshore of Abu Madafi and is not shown

1986). The four northern reefs instrumented in this study (Shi'b Nazar, Tahala, Al Degaig, and Abu Madafi, Fig. 1b) are best classified as table reefs, elongated in the alongshore dimension with a cross-shore scale of 100–500 m. The reefs in the Qita Dukais system are smaller, knoll-like platforms that are round or elliptical in shape and have no preferred orientation to the shoreline. Sea surface height fluctuates seasonally with wind patterns over the Red Sea (Sofianos and Johns 2001). Average water depth on the reef flat during the winter is approximately 1 and 0.5 m in the summer.

Experiment

The observations presented here are part of a larger, multi-year study of coral ecology, shelf-scale circulation, and air–sea dynamics in the Red Sea. We restrict our focus to measurements of meteorological conditions, currents, and water temperatures on nine offshore reef platforms (Tahala, Shi'b Nazar, Al Degaig, Abu Madafi, and five reefs in the Qita Dukais system) and the surrounding shelf (see Fig. 1b) collected from October 2008 to May 2010.

Temperature was measured on all reef flats, with the exception of Shi'b Nazar, using Onset Computer Corporation's HOBO U22 Water Temp Pro sensors attached to a small lead weight and placed on the bottom by a snorkler. Onset Temp Pros have a stated accuracy of 0.2°C; however, with careful calibration in the laboratory, in situ comparisons to more accurate temperature sensors have shown that accuracy can be improved to 0.02°C. Table 1 details the number of sensors distributed on each reef. On Tahala, Al Degaig, and Abu Madafi reefs, two temperature sensors were placed on the offshore or wave-exposed side of the reef flat with two further sensors on the onshore or wave-protected side. Within the Qita Dukais reef system, temperature sensors were concentrated on two of the largest coral knolls ("QD1" and "QD2") and a few sensors were also placed on smaller reefs (see Fig. 6 for sensor distribution in the Qita Dukais reef system). In addition to temperature sensors, a 2-MHz Nortek AquaDopp Profiler and Seabird SBE-37 Microcat were placed on reef QD1 and later on QD2 to measure currents, temperature, and conductivity.

To characterize the environmental conditions on the shelf surrounding the reefs, vertical arrays of temperature sensors, including Seabird SBE-39s, Seabird SBE-37s, RBR-1060s, RBR-2050s (all measuring temperature to ±0.002°C), and Onset Temp Pros, were deployed on taut-line moorings on the forereefs of Shi'b Nazar, Tahala, Al Degaig, and Qita Dukais and on the outer shelf at Mooring K2, at which conductivity was also measured using SBE-37s. Vertical profiles of water velocity were measured with an upward-looking Teledyne RDI Acoustic Doppler Current Profiler (ADCP) mounted on a bottom tripod at the K2 site (Fig. 1; see mooring details in Table 1). Tidal analysis was performed using the MATLAB toolbox T_TIDE (Pawlowicz et al. 2002).

The meteorological data used in this study are taken from a surface buoy deployed in 700 m of water (about 30 km offshore of Abu Madafi) and a 9-m coastal meteorological tower located on the campus of the King Abdullah University of Science and Technology (KAUST). Both the surface buoy and tower carry improved meteorological (IMET) sensor suites for measuring wind speed and direction, air temperature, relative humidity, barometric pressure, incoming shortwave radiation, incoming longwave radiation, and precipitation, which allow for estimates of the air–sea exchange of heat, freshwater, and momentum (Hosom et al. 1995; Colbo and Weller 2009).

Table 1 Details of moored instrumentation

Mooring type	Location	Water depth	Sensors
Shi'b Nazar Reef			
Vertical taut-line mooring on the forereef	22°19.853′N 38°51.117′E	16.7 m	Eight temperature sensors on vertical array from 1.8 to 15.7 meters depth
Tahala Reef			
Vertical taut-line mooring on the forereef	22°15.688′N 39°02.824′E	19.0 m	Five temperature sensors on vertical array from 2.1 to 18 meters depth
Reef platform instruments	22°15.772′N 39°03.093′E	0.8–1.0 m	Four Onset Temp Pro sensors spread across reef platform from April to October 2009
Al Degaig Reef			
Reef platform instruments	22°12.960′N 38°59.202′E	0.6–0.9 m	Four Onset Temp Pro sensors spread across reef platform from October 2008 to October 2009
Abu Madafi Reef			
Vertical taut-line mooring on the forereef	22°04.485′N 38°46.226′E	16.6 m	Six temperature sensors on vertical array from 2.2 to 16 meters depth 1,200 kHz ADCP, upward looking from a tripod
Reef platform instruments	22°04.312′N 38°46.238′E	0.7–0.9 m	Four Onset Temp Pro sensors spread across reef platform from April to October 2009
Qita Dukais Reef System			
Vertical taut-line mooring on the forereef	21°57.575′N 38°50.200′E	19.6 m	10 temperature sensors on vertical array from 0.6 to 9.8 meters depth
Reef platform instruments	21°58.042′N	1.3 m	2 MHz Nortek AquaDopp Profiler and a Seabird SBE-37 MicroCat
	38°50.169′E	0.6–2.1 m	14 Onset Temp Pro sensors spread across five reef platforms from Oct. 2008 to April 2009 increased to 25 sensors from April 2009 to May 2010.
K2 (*Outer shelf*)			
Vertical taut-line mooring and current meter	21°56.729′N 38°46.827′E	48.3 m	17 temperature sensors on vertical array from 0.6 to 47.3 meters depth 600 kHz ADCP, mounted on a tripod, looking upward from the bed
Meteorological Measurements			
Meteorological Buoy	22°09.638′N 38°30.069′E	697 m	Measurements: barometric pressure, air temperature, relative humidity, wind speed and direction, shortwave radiation, longwave radiation, precipitation, sea surface temperature and salinity, wave height, period, and direction
Meteorological tower	22°17.823′N 39°05.567′E	On land	Measurements: barometric pressure, air temperature, relative humidity, wind speed and direction, shortwave radiation, and longwave radiation

For Reef Platform moorings, the location given is in the center of the reef platform and the depth represents the range of water depths in which the reef-top sensors were deployed

Additionally, SST (at 0.6 m depth) and surface wave height were measured at the buoy.

Heat budget analysis

Here, we present the equations and define the coordinate system for a heat budget analysis on a reef platform. The coordinate system is aligned with the shape of the reef platform, which can be approximated as an ellipse. The temperature balance on the reef can be represented as follows:

$$\frac{\partial \overline{T}}{\partial t} + \overline{u}_i \frac{\partial \overline{T}}{\partial x_i} = -\frac{\partial}{\partial x_i} \overline{u_i' T'} + S \qquad (1)$$

where we use the summation convention with the index $i = 1$–3 and a right-handed coordinate system is adopted with the principle axes defined by x_i: x, aligned with the minor axis of the elliptical reef shape and positive toward the back reef, y, aligned with the major axis of the reef, and z, positive upward. u_i represents the corresponding velocity components u, v, and w, and T is water temperature. Overbars denote time-averaged quantities (in the case of our calculations, 1-h averages), and primed values are the fluctuating components $\left(u_i = \overline{u}_i + u_i'; T = \overline{T} + T'\right)$. The terms on the left-hand side of Eq. 1 represent the rate of change of temperature and the divergence of the advective heat flux. The terms on the right-hand side represent turbulent heat flux (including unresolved heat fluxes—anything with time scales of less than an hour) and sources or sinks of heat (S), respectively. Current measurements were only collected at one location on top of the reef, and

thus we cannot directly calculate spatial gradients in the turbulent transport of heat. However, this term can be estimated from a gradient diffusion-type model:

$$\frac{\partial}{\partial x_i}\overline{u_i' T_i'} \sim \frac{\partial}{\partial x_i}\left(-K_i \frac{\partial \overline{T}}{\partial x_i}\right) \sim -K_i \frac{\partial^2 \overline{T}}{\partial x_i^2}, \quad (2)$$

where K_i is the turbulent diffusivity.

Using the parameterization in Eq. 2, $K_i \sim 0.1$–$1\ \mathrm{m^2\ s^{-1}}$ (Sundermeyer and Ledwell 2001; Jones et al. 2008b), and an estimate of spatial gradients in temperature across the reef derived from observations on the most densely instrumented reef platforms in the Qita Dukais system, we estimate turbulent heat flux to be more than an order of magnitude smaller than the advective or surface heat flux. This is not sufficient justification for neglect of this term, especially since it seems likely that there will be times when turbulent heat flux will be of first-order importance. However, due to our inability to directly calculate turbulent heat flux, or alternatively, to have a better estimate of K_i, we will not include this term in the heat budget.

Vertically averaging Eq. 1 over the water column,

$$\langle T \rangle = \frac{1}{h}\int_0^h T dz; \langle u_i \rangle = \frac{1}{h}\int_0^h u_i dz, \quad (3)$$

neglecting the turbulent flux term, and multiplying by the heat capacity per unit volume (ρc_p, assumed constant and equal to $4.1 \times 10^6\ \mathrm{W\ s\ m^{-3}{}^{\circ}C^{-1}}$), gives an expression for the heat balance within a volume of water of unit length and width, with the top defined by the water surface ($z = h$) and bottom defined by the bed ($z = 0$):

$$\rho c_p h \frac{\partial \overline{\langle T \rangle}}{\partial t} = -\rho c_p h \langle \overline{u}_i \rangle \frac{\partial \overline{\langle T \rangle}}{\partial x_i} + Q_N + Q_{\mathrm{bed}}. \quad (4)$$

In the derivation of Eq. 4, we assume that water temperature is vertically uniform in the water column above the reef. Over a very rough coral bed, the vertical turbulent mixing is likely to be strong enough to maintain a nearly uniform temperature under most conditions. We tested this assumption using two temperature sensors on the reef flat separated vertically by 0.5 m and horizontally by 2 m, and they typically agreed to within the calibration uncertainty of the instruments. Eq. 4 also assumes that h does not vary spatially over the unit area or in time over the period of the calculation of these terms (1 h, in this case). The left-hand side of Eq. 4 represents the rate of change of heat storage within the volume (Q_T). The terms on the right-hand side of Eq. 4 are the advection of heat through the sides of the volume (ΔF) and the flux of heat through the water surface and the bed, respectively, and can be written as follows:

$$Q_T = \Delta F + Q_N + Q_{\mathrm{bed}}. \quad (5)$$

In this study, we assume that vertical advective heat flux due to groundwater movement and direct thermal conduction, Q_{bed}, is negligible, so that

$$Q_T = \Delta F + Q_N. \quad (6)$$

Net heat flux between the ocean and atmosphere, Q_N, is calculated as follows:

$$Q_N = Q_E + Q_H + Q_S + Q_L \quad (7)$$

where the terms on the right-hand side of Eq. 7 represent latent, sensible, net shortwave, and net longwave heat flux, respectively. Incoming shortwave radiation was corrected for surface reflection using an albedo that accounts for atmospheric transmittance (Payne 1972), plus an additional albedo (10%) to account for the reflectance of the coral bed in shallow water (Maritorena et al. 1994). Longwave, latent, and sensible heat fluxes were computed using a modified version 2.5 TOGA (Tropical Oceans Global Atmosphere) COARE (Coupled Ocean–Atmosphere Response Experiment) bulk algorithm (Fairall et al. 1996, 2003). Cool skin and warm layer corrections were not applied. ΔF is estimated from currents measured by the AquaDopp profiler on the reef flat and across-reef and along-reef temperature gradients, which are approximated by the centered difference of three reef-top temperature sensors aligned in each direction.

Results

Water temperature on the Red Sea reef platforms is spatially and temporally variable. Figure 2 illustrates the differences in water temperature on the wave-exposed and wave-protected sides of Abu Madafi reef, on the outer shelf, and Tahala reef, on the inner shelf, for a week in August 2009. This time series represents a period with some of the largest temperature variability in our observations. Water temperature on the side of the reefs protected from direct wave forcing has a larger diurnal range than on the wave-exposed side. For example, a coral on the wave-exposed side of the reef, which is regularly flushed with water from the shelf, may experience a diurnal temperature range of 0.5–1.5°C, while the same species on wave-protected side of the reef platform, approximately 200 m away, experiences a 2–5°C diurnal range.

Temperature variability across the shelf

Water temperature on the shelf surrounding the Red Sea reef platforms varied seasonally in 2009, with minimum temperatures near 25°C occurring between January and March and maximum temperatures above 32°C in late

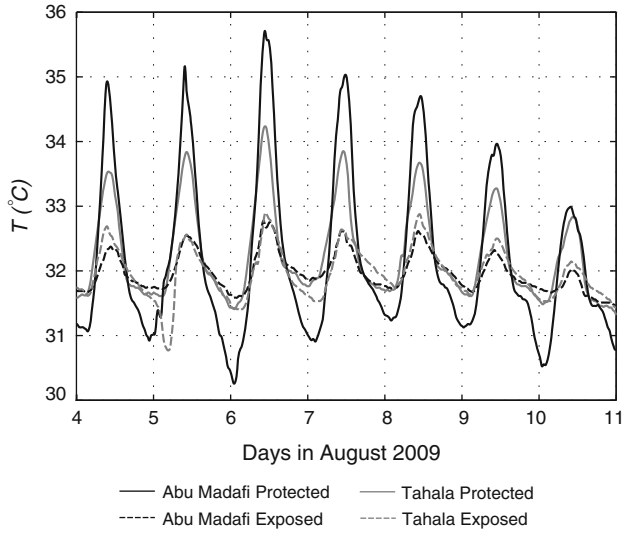

Fig. 2 Time series of water temperature on the wave-exposed and wave-protected sides of Abu Madafi and Tahala reefs during a week in summer 2009

August (Fig. 3). In late fall and winter, shelf water temperature decreases and there is relatively little stratification ($N^2 = 2 \times 10^{-5}$ s^{-2} on the forereef of Abu Madafi, where $N = \sqrt{-\frac{g}{\rho_0}\frac{\partial \rho}{\partial z}}$, ρ is potential density, ρ_0 is a reference density, g represents gravitational acceleration). During a period of steady cooling, from November 2008 to January 2009 (Fig. 3), inner shelf waters at Tahala are approximately a degree cooler than middle and outer shelf waters (Qita Dukais, Abu Madafi, Shi'b Nazar). In late spring and summer, shelf waters warm, stratification strengthens ($N^2 = 2 \times 10^{-4}$ s^{-2}), and inner shelf waters at Tahala are warmer than middle and outer shelf waters. Periods of cooling water temperatures, 1 to 3 weeks in duration, are superimposed on the annual temperature variation at all sites and may be due to wind-forced coastal upwelling on the eastern Red Sea shelf. An empirical orthogonal function (EOF) analysis of 33-h low-pass-filtered, depth-averaged water temperature on the forereefs of Shi'b Nazar, Tahala, Abu Madafi, and Qita Dukais reveals the spatial structure of the dominant mode, accounting for 97% of temperature variance, to be approximately uniform between the sites (not shown), suggesting that sub-diurnal frequency temperature variability is generally similar across the shelf.

While sub-diurnal temperature variability is fairly uniform across the shelf, diurnal oscillations in water temperature can look very different between sites. As an example, Fig. 4 presents week-long time series of water temperature at 0.6-m depth at the meteorological buoy and on the reef flat of QD1 in the Qita Dukais reef system for both winter and summer seasons. Temperatures on the reef have larger diurnal variations than surface temperature offshore. In the winter, the diurnal temperature variation on the reef can be fairly small, on the order of a 0.25–0.5°C, but in the summer, it can approach 6°C, when offshore surface waters vary only by 1.5–2°C. In the following section, we will show that there can be a significant amount of spatial variability in the thermal environment within the bounds of one reef platform.

Temperature variability on the reef platforms

The temperature of water on the reef platforms is influenced by seasonal cycles and synoptic wind-forcing events but also by small-scale circulation over and around the reef platforms, which controls the exchange of water with the surrounding shelf. Reef platforms rise sharply from the shelf to within a meter of the surface, and this inhomogeneity can lead to a high degree of spatial variability in the temperature field and the creation of thermal microclimates on the reef platform.

Circulation on the reef flat is largely wave-driven, with currents primarily to the southeast, in the direction of prevailing wind and waves. Previous studies have shown that waves break on the steeply sloping flanks of the reef, creating a spatial gradient in wave radiation stress and a superelevation of water level above the mean sea level (wave "setup"), driving flow over the shallow reef flat, from the reef crest to the backreef (Longuet-Higgins and Stewart 1964; Tait 1972; Symonds et al. 1995; Hearn 1999; Coronado et al. 2007; Hench et al. 2008). Significant wave height measured at the meteorological buoy ranged from less than 0.1–4.5 m with mean 0.94 ± 0.54 m. Currents measured on reef QD1 in the Qita Dukais reef system had a maximum speed of 25 cm s^{-1} and mean 8.8 ± 5.4 cm s^{-1}. Cross-reef currents on the reef were strongly correlated with offshore wave height ($r = 0.87$, P-value < 0.0001) but less correlated with eastward wind stress (approximately directed across the reef, $r = 0.50$, P-value < 0.0001) or wind stress magnitude ($r = 0.60$, P-value < 0.0001). While wave height is strongly coupled to wind stress magnitude in this region ($r = 0.80$, P-value < 0.0001), direct wind forcing on the reef, estimated from a simple balance between bottom stress and total wind stress (not shown), only accounts for reef currents on the order of a few cm s^{-1}. The tidal amplitude of sea surface height is 5–20 cm; however, a tidal analysis of currents measured in the center of the reef demonstrates that the tide explains less than 5% of the reef-top velocity variance.

An approximate estimate of the residence time of water on the reef can be calculated as $RT = V/Q$, where V is the volume of water on the reef and Q is the volumetric flow rate. V was estimated by approximating the reef as a 200- by 600-m rectangle with an average water depth of 1 m, and the volumetric flow rate was estimated from the

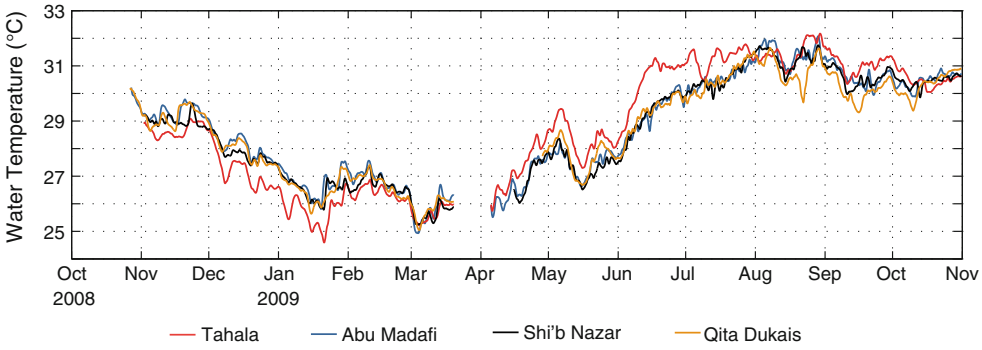

Fig. 3 Time series of depth-averaged water temperature, low-pass-filtered at a frequency corresponding to twice the local inertial period (32 h) at selected forereef moorings

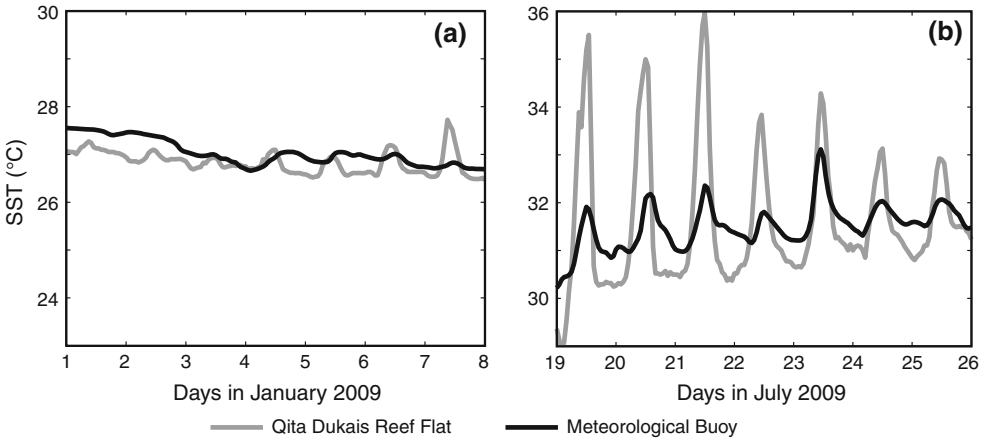

Fig. 4 Time series of water temperature at 0.6 m depth on Qita Dukais reef flat and at the Meteorological buoy offshore for a week in **a** winter–January 2009 and **b** summer–July 2009

velocity measured in the center of the reef (assumed to be representative of flow over the entire reef platform) and the cross-sectional area of the rectangular "reef". The average residence time of water on QD1 was approximately 100 min; however, depending on flow conditions, it can range from 10 min to several hours.

The simplified heat budget represented by Eq. 6 states that water temperature on the reef flat is determined by a balance between the transfer of heat at the air–water interface and the advection of heat by currents flowing over the reef. Thus, it is not surprising to find that the spatial variability of water temperature on the reef platforms, $\sigma_{T\text{-}spatial}$, calculated as the standard deviation of hour-averaged water temperature measured at all sensors on Qita Dukais at particular point in time, is related to the net surface heat flux, Q_N (Fig. 5a), as well as the magnitude of currents across the reef (Fig. 5b). $\sigma_{T\text{-}spatial}$ is maximized during periods of large, positive net surface heat flux and low currents. The strongest thermal gradients across the reef flat would be expected in the middle of the day during low-flow conditions, when both the surface heating potential and the residence time of water on the reef flat are maximized. While low-flow conditions are of great interest for the question of temperature variance on the reef flat, we do not include times when the flow is less than 2 cm s^{-1} in Fig. 5b, as this is approaching the uncertainty of the Nortek Aquadopp instrument. Moreover, we believe that in very sluggish flows, it is difficult to assume that flow measured at one point in the center of the reef is representative of flow across the entire reef platform.

Figure 6 shows the daily variability in water temperature at several sensors in the Qita Dukais reef system, estimated as the standard deviation of the 33-hr high-pass-filtered water temperature from June 2009 to May 2010, denoted by $\sigma_{T\text{-}diurnal}$. The greatest diurnal variation in water temperature occurs at sensors located in the center of the larger reef flats and on reefs protected from direct wave forcing, while sensors on smaller knolls or on the edges of the reef flat tend to experience less diurnal temperature variance.

A complicating factor in considering the spatial dependence of temperature variability across the reef is the dependence of the heat budget on water depth (seen explicitly in Eq. 4). Even on the reef flat, bathymetry is spatially variable. If we consider a situation in which there is no flow over the reef, for a given amount of surface heat flux acting on a unit area, a shallow site will heat faster during the day ($Q_N > 0$) and cool faster at night ($Q_N < 0$) than a deeper site. The maximum difference between the depths of temperature sensors on the reef bed was 1.9 m. Figure 7 illustrates a clear dependence of temperature variability on water depth for sensors on Qita Dukais, where the line represents the best fit to the observations. In addition to this depth dependence, however, a positional dependence is evident. The location of each reef flat

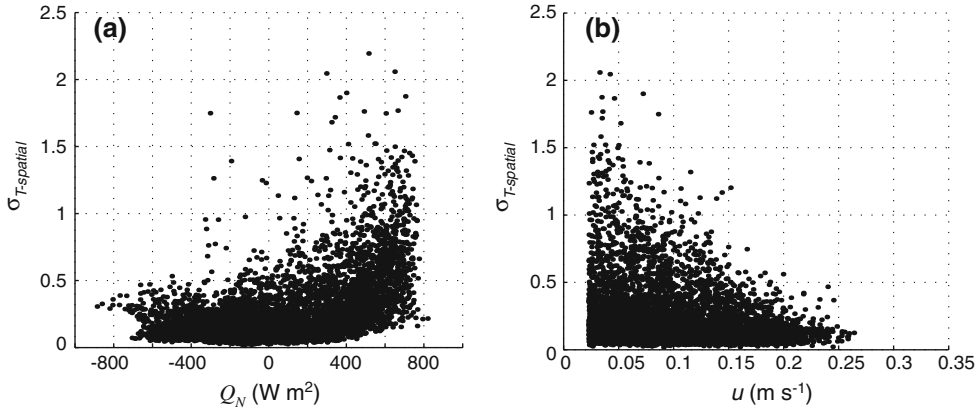

Fig. 5 The spatial standard deviation of water temperature at all sensors in the Qita Dukais reef system, $\sigma_{T\text{-}spatial}$, as a function of **a** net surface heat flux, Q_N, and **b** the magnitude of currents measured on the reef flat. Note that in panel (**b**), currents less than 2 cm s^{-1} have been excluded due to instrument accuracy

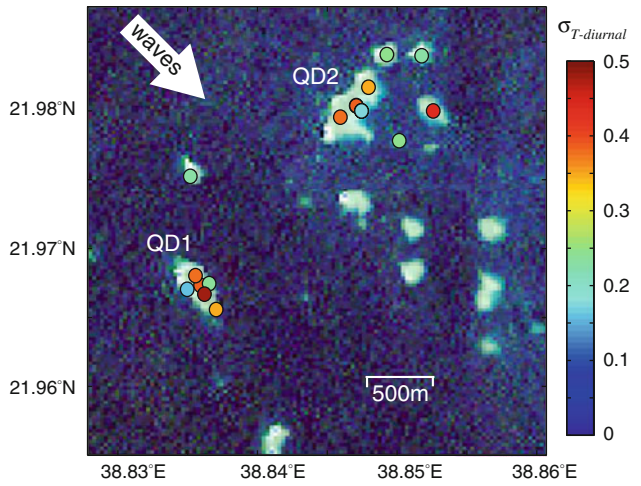

Fig. 6 USGS LandSAT image of Qita Dukais reef system. *Circles* show the location of Onset Temp Pros on the reef knolls and the color represents diurnal temperature variability at each location, estimated as, $\sigma_{T-diurnal} = \sigma\left(T_{33hr-hpf}\right)$, the standard deviation of the 33-h high-pass-filtered temperature

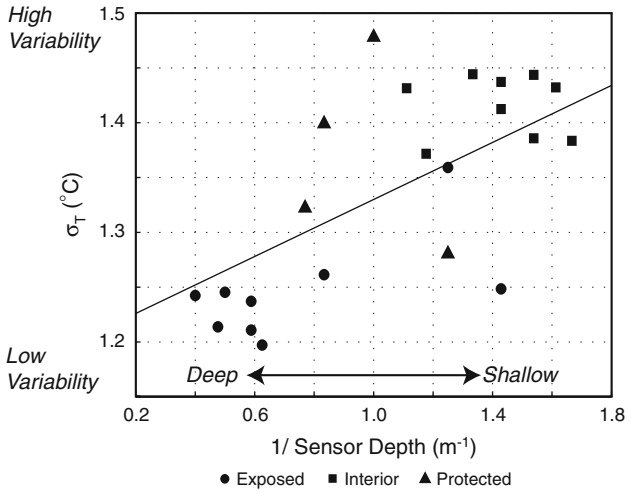

Fig. 7 The depth dependence of the standard deviation of temperature at each sensor in the Qita Dukais reef system. Markers represent the location of the sensor on the reef flat

measurement site was classified as "wave exposed" (within approximately 50 m of the offshore edge of the reef flat), "wave protected" (within approximately 50 m of the onshore edge of the reef flat), or "interior" (sensors not included in first two categories) and is indicated with data markers in Fig. 7. "Wave-exposed" sites are clustered below the best-fit line, whereas sensors in the interior of the reef flat and in "wave-protected" locations tend to fall above the best-fit line, suggesting an additional dependence of position on the temperature variance at each sensor.

Discussion

Heat balance over a reef platform

To examine the physical processes shaping the thermal environment on reef platforms in the Red Sea, a simple heat budget analysis (Eq. 6) was performed using a year of observations taken on QD1 and 8 months of data taken on QD2 in the Qita Dukais reef system (Fig. 6). Surface heat flux, estimated from Eq. 7 using meteorological observations from the offshore buoy and water temperature on the reef, is shown in Fig. 8a as a composite diurnal cycle (averaged over every hour of the day from October 2008 to October 2009, denoted as $\langle\rangle_d$). $\langle Q_N\rangle_d$ peaks mid-day at over 500 W/m^2 and is negative at night. A diurnal composite of the cross-reef component of current (Fig. 8b) shows that flow is, on average, directed onshore and is greatest in the afternoons, when the onshore component of wind is strongest (sea breeze; Fig. 8c) and wave height is maximized (Fig. 8d). Figure 8e shows the diurnal composite average water temperature in the interior of reef QD1. $\langle T\rangle_d$ increases just after sunrise, peaks in the early afternoon, after maximum surface heat flux, and then cools in the late afternoon and throughout the night.

The last panel in Fig. 8 shows a composite average of the observed rate of temperature change ($\langle \partial T/\partial t \rangle_d$; black line) and the contribution to the rate of temperature change from surface heat flux,

$$\left\langle \frac{Q_N}{\rho_0 c_p h} \right\rangle_d \text{(blue line)}, \tag{8}$$

pure advection,

$$-\left\langle u\frac{\partial T}{\partial x} + v\frac{\partial T}{\partial y} \right\rangle_d \text{(green line)}, \tag{9}$$

and both terms,

$$\left\langle \frac{Q_N}{\rho_0 c_p h} \right\rangle_d - \left\langle u\frac{\partial T}{\partial x} + v\frac{\partial T}{\partial y} \right\rangle_d \text{(red line)}. \tag{10}$$

Figure 8e illustrates that considering only surface heat flux (Eq. 8) results in an overestimate of the rate of temperature change on the reef, predicting more heating during the day and more cooling at night than is observed. In contrast, the rate of temperature change that would result from pure advection (Eq. 9), is positive at night, when $\partial T/\partial x$ is negative (because water on the shallow platform is cooler than the offshore water that is driven onto the reef by waves), and then becomes negative during the day, when the temperature gradient across the reef reverses (water on the reef is warmer than just offshore). The approximate balance of surface heat flux (blue) and advective (green) terms suggests that advection acts to relax the gradients in temperature set up by the surface heat flux. When both terms are used to estimate the rate of temperature change on the reef (Eq. 10), the resulting composite average has a shape very similar to the observations, explaining 93% of the variance in the diurnal composite averaged temperatures on the reef,

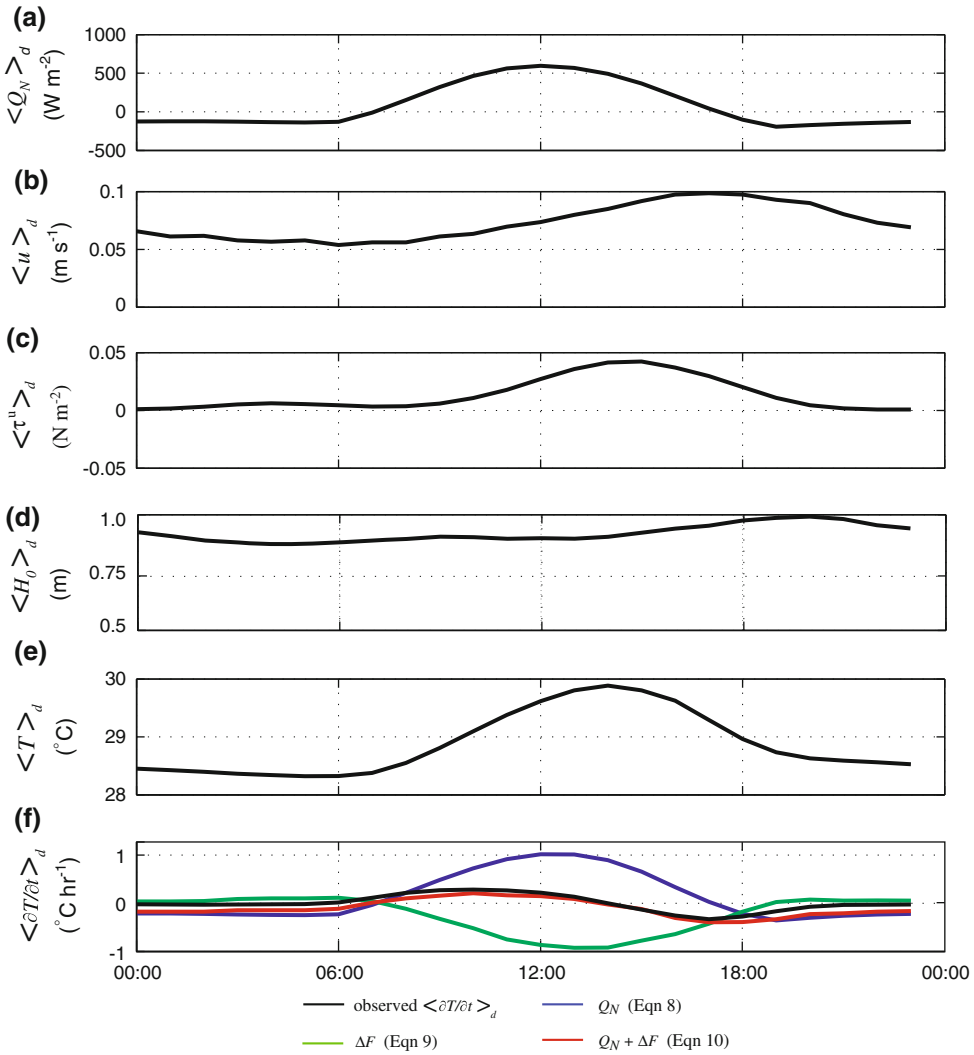

Fig. 8 Diurnal composite average (October 2008–October 2009) of **a** net surface heat flux, **b** across-reef current measured on reef QD1, **c** across-shore wind stress, **d** significant wave height measured at meteorological buoy, **e** temperature at a sensor in the interior of QD1, and **f** the observed and predicted rate of change of temperature. Legend applies to **f**

with a residual (model minus observed) of 0.13°C h^{-1}. The primary disparity between Eq. 10 and the observations occurs at night—the model predicts more heat loss than is observed. In general, the simple model represented by Eq. 10 has skill representing the observations averaged over the whole year and performs similarly well on seasonally averaged data (winter or summer) (Fig. 9).

Figure 9 presents a comparison of hour-averaged surface heat flux and advective terms calculated from the October 2008–October 2009 deployment on reef QD1 and the November 2009–May 2010 deployment on reef QD2 (see Fig. 6). The data shown here are restricted to times when flow on the reef was greater than 2 cm s^{-1}. A linear fit to the observations demonstrates a strong relationship ($r = 0.83$, P-value < 0.0001) between surface heat flux and advective terms with a slope of 0.97.

A simple conceptual model of the processes controlling the diurnal temperature variations over the reef is summarized in Fig. 10. Waves breaking on the steep forereef create a wave setup on the wave-exposed side of the reef. The pressure head from the wave setup drives flow over the reef from the wave-exposed side to the wave-protected side. We can imagine a parcel of water as it moves from the deep water offshore of the reef over the reef platform (from left to right in Fig. 10), in a Lagrangian reference frame. $\partial T/\partial t$ for the water parcel goes as Q_N/h (advection drops out in this reference frame); thus, as depth decreases over the shallow reef, the parcel of water heats up (or cools down) faster than over the deeper water offshore. Therefore, areas in the interior and on the protected side of the reef will experience much larger temperature extremes than areas on the forereef or wave-exposed side of the reef flat.

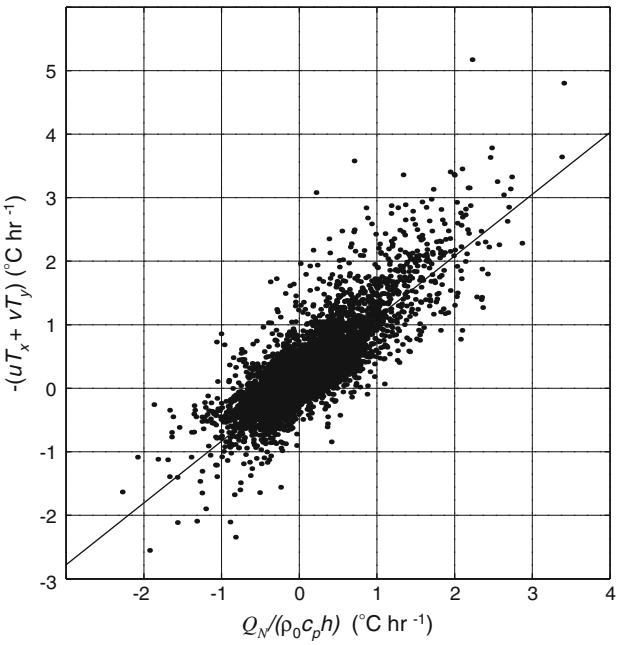

Fig. 9 Advection vs. surface heat flux terms of the heat budget (Eq. 6) calculated from the October 2008–October 2009 deployment on reef QD1 and the November 2009–May 2010 deployment on reef QD2

We can further test the skill of this simple model by predicting the temperature on reef platforms for which we do not have current measurements. From April–October 2009, temperature measurements were collected on the wave-exposed (offshore) and wave-protected (onshore) sides of Abu Madafi, Al Degaig, and Tahala reefs. Figure 11 shows an estimate of the temperature difference across each reef estimated from a simple heat budget model

$$\Delta T_{HBM} = \frac{Q_N \Delta x}{\rho_0 c_p h u} \tag{11}$$

where h was chosen to be the spatially averaged water depth at the sensor locations on each reef as measured in October 2009, versus the observed difference in temperature between the sensors averaged over 1 h, ΔT_{obs}. In Eq. 11, u is the across-reef component of flow, determined from an empirical relationship with offshore significant wave height, $u = 0.06H_0$, which was derived from the current measurements on reefs QD1 and QD2 ($r = 0.77$, P-value < 0.0001). The skill of the simple heat budget is fairly good at Abu Madafi (located on the outer shelf), giving a standard error of 0.2°C. However, the skill decreases toward the inner shelf (standard error of 0.4°C at Tahala), which is likely due to the fact that the empirical relationship used to estimate u was derived on a reef that is exposed to offshore waves (Qita Dukais reef system), and the wave heights measured offshore at the meteorological buoy are less representative of the waves incident on the protected reefs.

Conclusions

In 2009 and 2010, temperature variability on Red Sea reef platforms was dominated by diurnal variability. The daily temperature range on the reefs, at times, exceeded 5°C—as large as the annual range of water temperature on the shelf. The shallow topography of the reef platforms enhances the diurnal temperature cycle by concentrating the effect of surface heat flux into a small volume of water and by exposing the reef flat to direct wind and wave forcing, all of which have diurnal variability. The topographic complexity of the reefs also leads to a high degree of temperature variability at small spatial scales, with cooler temperatures on the forereef or wave-exposed side of the reef and warmer temperatures in the reef interior and on the wave-protected side of the reef. The existence of thermal microclimates on reef platforms may result in

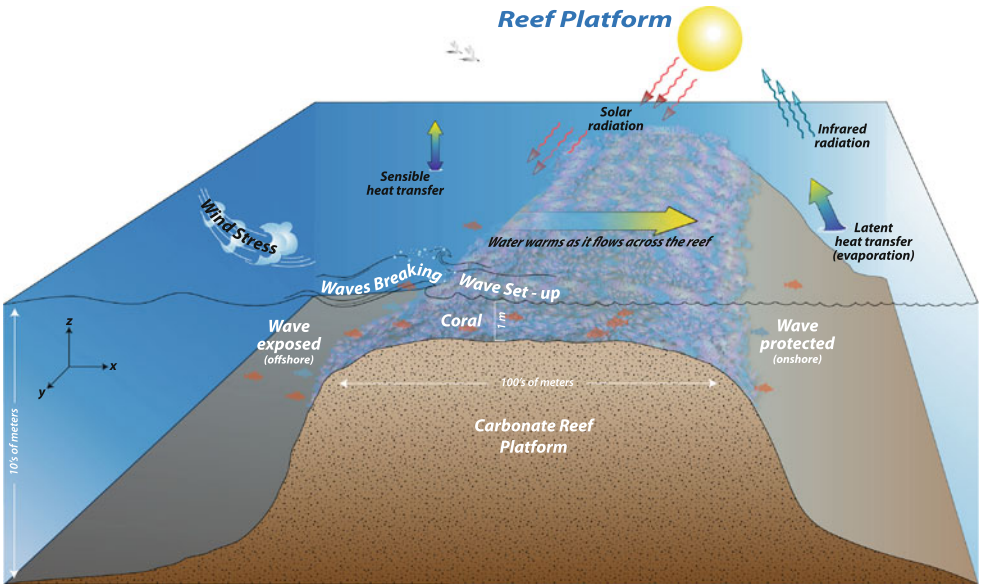

Fig. 10 Conceptual illustration of a reef platform and the physical processes that shape the thermal environment

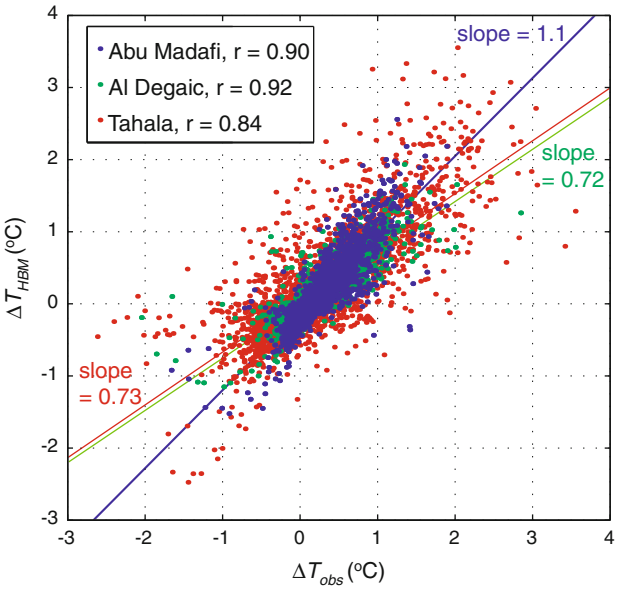

Fig. 11 Across-reef temperature gradient predicted by a simple heat budget model (ΔT_{HBM}) versus the observed temperature gradient (ΔT_{obs}) on Abu Madafi, Al Degaig, and Tahala. Regression slopes are indicated next to best-fit lines for each reef

colonies with different physiology and diverse coral symbiont assemblages.

We found that the temporal (Fig. 8) and spatial (Fig. 11) variability in water temperature on the reef platforms can be fairly well predicted by a simplified heat budget, which includes the transfer of heat at the air–water interface and the advection by currents flowing over the reef. With this simple model, we predicted the temperature difference across three reefs to within 0.4°C on the outer shelf and 0.9°C on the inner shelf (95% confidence) using only information about bathymetry, surface heat flux, and offshore wave conditions, the last two of which were measured at the meteorological buoy for this study, but could be obtained from remote sensing products or coastal weather stations. The results of this work have implications for improving indices of coral bleaching, which typically have difficulty predicting the high degree of spatial variability observed at global, regional, and individual reef scales. The incorporation of a simple heat budget model into the coral bleaching indices could help to capture the effect of wave-driven circulation on the thermal environment of reefs.

Acknowledgments The authors would like to thank A. Al Suwailem, Y. Kattan, H. Al Jahdali, W. Moazen, and Nageeb from King Abdullah University of Sciences and Technology (KAUST) for providing logistical and field support, C. Marquette, S. Elgar, L. Gorrell, and D. Ralston from WHOI for equipment and technical support, E. Paul Oberlander for the artistic rendering of Fig. 10, as well as three anonymous reviewers for their thoughtful comments. This publication is based on work supported by Award No. USA 00002/KSA 00011 made by King Abdulla University of Science and Technology (KAUST). K. A. D. was supported by a USGS postdoctoral scholarship at WHOI.

References

Berkelmans R (2002) Time-integrated thermal bleaching thresholds of reefs and their variation on the Great Barrier Reef. Mar Ecol Prog Ser 229:73–82

Bird JC (2005) Modelling sub-reef thermodynamics to predict coral bleaching: a case study at Scott Reef, WA. MSc Thesis, James Cook University, p 156

Buddemeier RW, Fautin DG (1993) Coral bleaching as an adaptive mechanism. Bioscience 43:320–326

Cantin NE, Cohen AL, Karnauskas KB, Tarrant AM, McCorkle DC (2010) Ocean warming slows coral growth in the Central Red Sea. Science 329:322–325

Colbo K, Weller RA (2009) Accuracy of the IMET sensor package in the subtropics. J Atmos Oceanic Technol 26:1867–1890

Coronado C, Candela J, Iglesias-Prieto J, Sheinbaum J, López M, Ocampo-Forres F (2007) On the circulation in the Puerto Morelos fringing reef lagoon. Coral Reefs 26:146–163

Ekman VW (1905) On the influence of the Earth's rotation on ocean-currents. Arkiv for Matematik, Astronomi och Fysik 2:1–53

Fairall CW, Bradley EF, Rogers DP, Edson JB, Young GS (1996) Bulk parameterization of air-sea fluxes for tropical ocean-global atmosphere coupled-ocean atmosphere response experiment. J Geophys Res 101:3747–3764

Fairall CW, Bradley EF, Hare JE, Grachev AA, Edson JB (2003) Bulk parameterization of air-sea fluxes: updates and verification for the COARE algorithm. J Clim 16:571–591

Glynn PW (1993) Coral reef bleaching: ecological perspectives. Coral Reefs 12:1–17

Glynn PW, Maté JL, Baker AC, Calderón MO (2001) Coral bleaching and mortality in Panama and Ecuador during the 1997–1998 El Nino-Southern Oscillation Event: Spatial/temporal patterns and comparisons with the 1982–1983 event. Bull Mar Sci 69:79–109

Goreau T, McClanahan T, Hayes R, Strong A (2000) Conservation of coral reefs after the 1998 global bleaching event. Conserv Biol 14:5–15

Guinotte JM, Buddemeier RW, Kleypas JA (2003) Future coral reef habitat marginality: temporal and spatial effects of climate change in the Pacific basin. Coral Reefs 22:551–558

Hearn CJ (1999) Wave-breaking hydrodynamics within coral reef systems and the effect of changing relative sea level. J Geophys Res 104:30,007-030,019

Hench JL, Leichter JJ, Monismith SG (2008) Episodic circulation and exchange in a wave-driven coral reef and lagoon system. Limnol Oceanogr 53:2681–2694

Hoegh-Guldberg O (1999) Climate change, coral bleaching and the future of the world's coral reefs. Mar Freshw Res 50:839–866

Hosom DS, Weller RA, Payne RE, Prada KE (1995) The IMET (improved meteorology) ship and buoy systems. J Atmos Oceanic Technol 12:527–540

Jiang H, Farrar JT, Beardsley RC, Chen R, Chen C (2009) Zonal surface wind jets across the Red Sea due to mountain gap forcing along both sides of the Red Sea. Geophys Res Lett 36:L19605, 6 pp

Jones AM, Berkelmans R, MJHv Oppen, Mieog JC, Sinclair W (2008a) A community change in the algal endosymbionts of a scleractinian coral following a natural bleaching event: field evidence of acclimatization. Proc R Soc Biol Sci Ser B 275:1359–1365

Jones NL, Lowe RJ, Pawlak G, Fong DA, Monismith SG (2008b) Plume dispersion on a fringing coral reef system. Limnol Oceanogr 53:2273–2286

Lesser MP, Mazel CH, Gorbunov MY, Falkowski PG (2004) Discovery of symbiotic nitrogen-fixing cyanobacteria in corals. Science 305:997–1000

Longuet-Higgins MS, Stewart RW (1964) Radiation stresses in water waves; a physical discussion, with applications. Deep Sea Res 11:529–562

Maritorena S, Morel A, Gentili B (1994) Diffuse reflectance of oceanic shallow waters: influence of water depth and bottom albedo. Limnol Oceanogr 39:1689–1703

McClanahan TR, Maina J, Moothien-Pillay R, Baker AC (2005) Effects of geography, taxa, water flow, and temperature variation on coral bleaching intensity in Mauritius. Mar Ecol Prog Ser 298:131–142

Montaggioni LF, Behairy AKA, El-Sayed MK, Yusuf N (1986) The modern reef complex, Jeddah area, Red Sea: a facies model for carbonate sedimentation on embryonic passive margins. Coral Reefs 5:127–150

Nadaoka K, Nihei Y, Kumano R, Yokobori T, Omija T, Wakaki K (2001) A field observation on hydrodynamic and thermal environments of a fringing reef at Ishigaki Island under typhoon and normal atmospheric conditions. Coral Reefs 20:387–398

Nakamura T, van Woesik R (2001) Water-flow rates and passive diffusion partially explain differential survival of corals during the 1998 bleaching event. Mar Ecol Prog Ser 212:301–304

Oliver TA, Palumbi SR (2009) Distributions of stress-resistant coral symbionts match environmental patterns at local but not regional scales. Mar Ecol Prog Ser 378:93–103

Palardy JE, Rodrigues LJ, Grottoli AG (2008) The importance of zooplankton to the daily metabolic carbon requirements of healthy and bleached corals at two depths. J Exp Mar Biol Ecol 367:180–188

Pawlowicz R, Beardsley B, Lentz S (2002) Classical tidal harmonic analysis including error estimates in MATLAB using T_TIDE. Comput Geosci 28:929–937

Payne RE (1972) Albedo of the sea surface. J Atmos Sci 29:959–970

Riegl B, Piller WE (2003) Possible refugia for reefs in times of environmental stress. Int J Earth Sci (Geol Rundsch) 92:520–531

Sammarco PW, Winter A, Stewart JC (2006) Coefficient of variation of sea surface temperature (SST) as an indicator of coral bleaching. Mar Biol 149:1337–1344

Schiller A, Ridgway KR, Steinberg CR, Oke PR (2009) Dynamics of three anomalous SST events in the Coral Sea. Geophys Res Lett 36

Skirving W, Heron M, Heron S (2006) The hydrodynamics of a bleaching event: implications for management and monitoring. In: Phinney JT, Hoegh-Guldberg O, Kleypas J, Skirving W, Strong A (eds) Coral reefs and climate change—science and management. American Geophysical Union, Washington, pp 145–161

Smith NP (2001) Weather and hydrographic conditions associated with coral bleaching: Lee stocking Island, Bahamas. Coral Reefs 20:415–422

Sofianos SS, Johns WE (2001) Wind induced sea level variability in the Red Sea. Geophys Res Lett 28:3175–3178

Sofianos SS, Johns WE (2002) An oceanic general circulation model (OGCM) investigation of the Red Sea circulation, 1: exchange between the Red Sea and the Indian Ocean. J Geophys Res 107:3196

Sofianos SS, Johns WE (2007) Observations of the summer Red Sea circulation. J Geophys Res 112:C06025, 20 pp

Sundermeyer MA, Ledwell JR (2001) Lateral dispersion over the continental shelf: analysis of dye release experiments. J Geophys Res 106:9603–9621

Symonds G, Black KP, Young IR (1995) Wave-driven flow over shallow reefs. J Geophys Res 100:2639–2648

Tait RJ (1972) Wave set-up on coral reefs. J Geophys Res 77: 2207–2211

Weller E, Nunez M, Meyers G, Masiri I (2008) A climatology of ocean-atmosphere heat flux estimates over the Great Barrier Reef and Coral Sea: implications for recent mass coral bleaching events. J Clim 21